TDA Progress Report 42-102

August 15, 1990

Navigational Utility of High-Precision Radio Interferometry for Galileo's Approach to Jupiter

W. M. Folkner
Tracking Systems and Applications Section

The effect of very long baseline interferometry (VLBI) measurements of 2-nanoradian (nrad) accuracy has been studied for use in Galileo's approach to Jupiter's moon Io. Of particular interest is reducing the error in the minimum altitude above Io's surface. The nominal tracking strategy includes Doppler, range, and onboard optical data, in addition to VLBI data with 25-nrad accuracy. For nominal data, the altitude error is approximately 250 km with a data cutoff of 19 days before closest approach to Io. A limited number (two to four) of 2-nrad VLBI measurements, simulating a demonstration of improved VLBI data, were found to reduce the altitude error by 10 to 40 percent. Improving the accuracy of the VLBI measurements of the nominal tracking strategy to 2 nrads, to simulate the results from an operational few-nrad VLBI capability, was found to reduce the altitude error by an approximate factor of four. This reduction in altitude error is attributed to the ability that VLBI data give to help determine the along-track component of Jupiter's ephemeris. This capability complements the ability of the onboard optical data to determine the radial and cross-track components of Jupiter's ephemeris.

I. Introduction

Angular tracking through very long baseline interferometry (VLBI) has been routinely performed for the Voyager spacecraft [1] and is planned for the Galileo spacecraft. Using a technique called delta differential one-way ranging (ΔDOR), the geometric delay of a radio signal from the spacecraft between two tracking stations is differenced with the delay of the signal from a nearby natural radio source. This difference provides a measurement of the angle between the spacecraft and the radio source. A ΔDOR measurement along one baseline determines one component of the angular plane-of-sky spacecraft position. Measurements on two nearly orthogonal baselines can provide complete plane-of-sky position information. The accuracy of the ΔDOR measurement is about 50 nrad for the Voyager spacecraft and is expected to be about 25 nrad for the Galileo spacecraft using the present operational VLBI system.[1] An angular accuracy of 25 nrad corresponds to about 20 km over the Earth–Jupiter distance.

[1] J. B. Thomas, "An Error Analysis for Galileo Angular Position Measurements with the Block I ΔDOR System," JPL Engineering Memorandum No. 335-26 (internal document), Jet Propulsion Laboratory, Pasadena, California, November 11, 1981.

Improved VLBI technology promises to provide more accurate angular-position measurements. Specifically, the local-reference-frame technique [2] uses scans of the spacecraft and multiple radio sources to cancel many error sources. The resulting angular accuracy could reach the 2-nrad level. This order-of-magnitude improvement in VLBI measurement capability will not necessarily result in a similar orbit determination improvement. Other data, such as onboard optical data, may provide information that makes the VLBI data redundant. Random forces, due to solar pressure or gas leaks, may limit the utility of the improved VLBI data.

In order to study quantitatively the effect of high-precision VLBI measurements on orbit determination, a covariance study was performed on the approach of the Galileo spacecraft to Jupiter. This case was chosen since earlier analyses[2] [3] indicated that the VLBI data could improve orbit determination by reducing uncertainty about the Jovian ephemeris. This is accomplished by detecting the planet's gravitational signature on the motion of the spacecraft. The present study, while specific, extends the previous analyses by utilizing the full Orbit Determination Program (ODP), including random-force models and onboard optical data.

Starting from the previous work of Pollmeier,[3] covariance analyses were performed to examine how high-precision ΔDOR measurements might affect the expected orbit-determination accuracy. For this study, the high-precision ΔDOR measurements were treated as regular ΔDOR measurements with improved accuracy. Three groups of cases are presented here. The first group examines the effect of a limited number (two to four measurements per baseline) of high-precision ΔDOR measurements. These are in addition to the nominal radio metric and optical data on the standard Galileo orbit determination. These few measurements could be included in an orbit analysis to provide a demonstration of the local-reference-frame technique. They also could be included in a post-encounter analysis to evaluate the accuracy of the local-reference-frame technique for spacecraft navigation. One case considered by Pollmeier includes increased Doppler accuracy, which would be attained using an X-band (8.1-GHz) uplink instead of the nominal S-band (2.3-GHz) uplink, for improved orbit determination. The second group of cases included in this study evaluates the effect of adding a limited number of high-precision ΔDOR measurements to this improved Doppler data. For the final cases, all normally scheduled ΔDOR measurements are treated as high-precision measurements, as though the local-reference-frame technique was an operational capability. While this is not likely to be true of Galileo's Jupiter approach, it serves to show the potential of improved VLBI-tracking data.

II. Trajectory and Mapping

These analyses are based on the trajectory for the Io encounter, scheduled to take place on December 7, 1995.[4] Figure 1 is a plot of the approach trajectory in the ecliptic plane as seen by an inertial observer. Jupiter is traveling from left to right catching up to the spacecraft. The points are shown at four-hour intervals. Figure 2 is a plot of the approach trajectory in the ecliptic plane centered on Jupiter with points at one-hour intervals. Galileo makes a close encounter with Jupiter's moon Io approximately five hours before closest approach to Jupiter. The Io encounter is used to provide a gravitational assist in establishing the Jupiter-centered orbit. A major navigation requirement is that Galileo remain 500 km or higher above the surface of Io to avoid possible collision with volcanic ejecta. The trajectory design has Galileo pass 1000 km above Io. Consultations with the Galileo orbit determination team of F. T. Nicholson, D. W. Murrow, and V. M. Pollmeier suggest that there are two times when additional accuracy will be desired, namely at the 26-hour data cutoffs preceding trajectory correction maneuvers TCM-27 and -28. These cutoffs occur at Io–19 days 2 hours and at Io–11 days 2 hours.

For local-reference-frame measurements, a number of quasars are needed about the spacecraft. Figure 3 is a plot of the spacecraft trajectory in the plane of the sky with points at four-day intervals. The low declination of the approach trajectory will cause observations at the Goldstone and Madrid sites to be at low elevation. This will restrict the choice of quasars for the local reference frame and may reduce the accuracy of local-reference-frame ΔDOR measurements. Three of the radio sources shown in Fig. 3

[2] R. N. Treuhaft and J. S. Ulvestad, "Using Gravitational Signatures for Target-Relative Angular Tracking During Planetary Approach," JPL Interoffice Memorandum 335.3-88-76 (internal document), Jet Propulsion Laboratory, Pasadena, California, July 11, 1988.

[3] V. M. Pollmeier, "Io Delivery Uncertainties and Parametric Variation Studies for the Jupiter Approach of the October 10 Gaspra Ida Trajectory," JPL Interoffice Memorandum GLL-NAV-89-31 (internal document), Jet Propulsion Laboratory, Pasadena, California, March 16, 1989.

[4] J. R. Johannesen, "Reference Integrated Interplanetary, Probe, and Orbiter Trajectories for the 1989 VEEGA with Gaspra and Ida Asteroid Flyby," JPL Interoffice Memorandum 312-88.4-1461 (internal document), Jet Propulsion Laboratory, Pasadena, California, April 25, 1988.

are from the Magellan catalog[5] with the remainder from a VLBI survey [4].

The initial spacecraft state was specified at Io encounter minus 142 days, which is after the separation of the probe from the orbiter and after the orbit-deflection maneuver (ODM). Maneuvers included in this analysis are the ODM-cleanup maneuver (TCM-26) at encounter minus 100 days and trajectory-correction maneuvers, TCM-27 and -28. The orbit-determination results are mapped to the Io-centered B-plane coordinate system[6] referred to the Jupiter mean equator of 1950 at time of closest approach to Io. Since the spacecraft trajectory lies mainly in Jupiter's equatorial plane and is not greatly deflected by Io, the B-plane component $B \cdot T$ corresponds within a few percent to the distance from the center of Io. The $B \cdot T$ error corresponds to the error in altitude above Io, which is the error of interest.

III. Error Modeling

The error modeling used here is adopted from Pollmeier.[7] In the covariance analysis, many parameters are estimated along with the spacecraft state while other parameters are considered. In a consider analysis [5], errors in estimated parameters due to (nonestimated) considered parameters are added (in quadrature) to the computed error (which resulted from data noise and a priori errors in the estimated parameters) to form the total error. An error from a considered parameter which forms a large portion of the total error may indicate a need for a different error modeling for that parameter. The estimated and considered parameters for the standard cases are listed in Table 1 along with a priori error information. The diagonal components of the covariance matrices for the Earth–Jupiter ephemeris,[8] the Galilean satellite ephemerides,[9] and the station locations[10] are listed in Table 1. Since the ephemerides are estimated and only one quasar is used for ΔDOR measurements, the quasar can be used to define the orientation of the reference frame. If more than one quasar were used, a relative quasar location error would have to be included.

The standard data types are S-band two-way Doppler and range, X-band VLBI data, and onboard optical data. The nominal data schedule is outlined in Table 2. The minimum elevation for radio metric data is 15 deg for range and Doppler and 7 deg for ΔDOR. Radio metric data are taken more often just after the probe release (Io–142 to Io–136), around the ODM-cleanup maneuver at Io–100 days, and from Io–60 days to encounter.

For the purpose of the local-reference-frame ΔDOR demonstration, an additional set of measurements was scheduled with two points for each of the Goldstone–Canberra and Goldstone–Madrid baselines in the week preceding TCM-27 and two more per baseline between TCM-27 and -28. The times, shown in Table 3, were chosen to allow about two days of processing time prior to the data cutoffs. When included, these measurements were independently weighted and merged with the rest of the data set. The high-precision ΔDOR measurements were weighted at either 3 cm or 1 cm (corresponding to a 100-psec or 33-psec delay error). The plane-of-sky angular error depends on the projected baseline length. For example, a 1-cm ΔDOR error and a 5000-km projected baseline correspond to 2-nrad angular accuracy.

Station-location and media errors, which are treated as consider parameters for ΔDOR measurements, are estimated in the local-reference-frame technique. For cases which included only a limited number of high-precision ΔDOR measurements, the station-location and media errors did not significantly contribute to the total orbit-determination error. But when all ΔDOR measurements were treated as high precision, analyses were done both with the standard considered-error models (with station-location and media errors for the ΔDOR measurements considered) and with modified error modeling (with station-location and media errors for ΔDOR measurements removed).

---

[5] J. S. Ulvestad and O. J. Sovers, "Preliminary VLBI catalog for Magellan," JPL Interoffice Memorandum 335.3-89-14 (internal document), Jet Propulsion Laboratory, Pasadena, California, January 30, 1989.

[6] For a description of the B-plane coordinate system, see G. W. Spier, "Design and Implementation of Models for the Double Precision Trajectory Program (DPTRAJ)," JPL Technical Memorandum 33-451 (internal document), Jet Propulsion Laboratory, Pasadena, California, pp. 103-116, 1971.

[7] V. M. Pollmeier, op. cit.

[8] E. M. Standish, "The Covariance of Venus, Jupiter, and the Earth," JPL Interoffice Memorandum 314.6-969 (internal document), Jet Propulsion Laboratory, Pasadena, California, June 1, 1988.

[9] D. W. Murrow, "A Covariance for the Galilean Satellites for ODP Analysis," JPL Interoffice Memorandum 314.3-771 (internal document), Jet Propulsion Laboratory, Pasadena, California, November 5, 1987.

[10] D. W. Murrow and F. T. Nicholson, "Station Location Covariance," JPL Interoffice Memorandum GLL-NAV-88-50 (internal document), Jet Propulsion Laboratory, Pasadena, California, September 2, 1988.

IV. Standard Case Results

Table 4 lists three sets of orbit-determination results at the Io–19- and –11-day cutoffs. All three sets include the standard error models and the nominal data outlined in the previous section. The set labeled Nominal includes 16 ΔDOR points per baseline for the Io–19-day cutoff and 18 ΔDOR points per baseline for the Io–11-day cutoff, but does not include high-precision ΔDOR data. The Demo-3-cm set includes the demonstration measurements from Table 3 weighted at 3 cm. The Demo-1-cm set includes the same demonstration measurements weighted at 1 cm.

The errors are tabulated in the Io-centered B-plane coordinate system for completeness. The impact parameter $\vec{B}$ has components $B \cdot T$, in the plane of the trajectory, and $B \cdot R$, perpendicular to the trajectory plane. Of particular interest is the error in altitude above Io, which corresponds to the column labeled $B \cdot T$. The linearized time of flight (LTOF) parameterizes the position along the trajectory. The LTOF error (in seconds) can be multiplied by the velocity at infinity,[11] 14.9 km/sec, to compare it to the impact-parameter errors $B \cdot R$ and $B \cdot T$. The LTOF error is thus the largest error by about 15 percent. Inclusion of more or better ΔDOR data will result in a comparable improvement in $B \cdot T$ and LTOF. That is, a reduction of 20 percent in the LTOF error is accompanied by a corresponding 20 percent reduction in the $B \cdot T$ error. This is because the dominant error is the Jupiter along-track error which projects by a fixed amount in the $B \cdot T$ and LTOF directions. The $B \cdot R$, which is perpendicular to the along-track error, is not affected much by improvements in the ΔDOR data since the onboard optical data provide better information in the cross-track direction.

The important error is the error in altitude above Io ($B \cdot T$ error) at the Io–19- and –11-day cutoffs. The Demo-3-cm set shows an altitude error improvement of 19 percent over the Nominal set at the Io–19-day cutoff and a 21 percent improvement at Io–11 days. The Demo-1-cm set shows an improvement of 36 percent over the Nominal set at Io–19 days and 38 percent at Io–11 days.

V. Demonstration of High-Precision ΔDOR with Improved Doppler Data

Since improved orbit-determination accuracy is desired over standard results, a case with improved Doppler data accuracy is being considered.[12] The improved Doppler accuracy would be achieved through use of an X-band uplink and downlink instead of the nominal S-band frequency. The cases presented here examine whether a demonstration of the high-precision ΔDOR system could yield a significant improvement in orbit-determination accuracy in the presence of improved Doppler data.

For these cases, Doppler accuracy was improved from 1 mm/sec to 0.2 mm/sec due to reduced instrumental errors for the higher-frequency link. The ionosphere errors were reduced by a factor of ten (from 75 to 7.5 cm) due to the $1/f^2$ behavior of the ionosphere delay. The improved Doppler accuracy increased the sensitivity of the orbit determination to station-location uncertainty. Rather than include a large considered station-location error, these cases used the improved Doppler data to estimate station locations. The data schedule was the same as for the standard cases.

Table 5 lists the results for the improved Doppler cases. The altitude error for Demo 3 cm is 14 percent lower than the Nominal case at Io–19 days and 11 percent lower at Io–11 days. The Demo-1-cm results are 29 percent lower than the Nominal at Io–19 days and 30 percent lower at Io–11 days.

VI. High-Precision ΔDOR as an Operational Data Type

If high-precision ΔDOR is demonstrated to be a viable navigational tool, it will be possible to schedule such measurements regularly during the approach phase of a mission. For the cases presented in Table 6, the ΔDOR measurements from Table 2, comprising VLBI measurements scheduled for mission navigation, were included with 1-cm weight. Demonstration measurements from Table 3 were not included. The weights for other data types were the same as in the standard case. The All-ΔDOR-1-cm set with standard models retains the same considered-error models for media, station locations, and quasar location as the regular ΔDOR measurements. The computed $B \cdot T$ error at the Io–19-day cutoff shows improvement by a factor of three over the standard-case result with Nominal data. The contribution of media errors for this case is nearly as large as the computed error. For local-frame measurements, media effects can be estimated separately and included in the measurement error. For the All-ΔDOR-1-cm case with modified models, the ODP was modified to ignore the considered media and station-location errors for the ΔDOR measurements while retaining those considered errors for the range and Doppler measurements. In this case, the considered errors are reduced and the total $B \cdot T$ error is smaller than the standard nominal case error by nearly a factor of four.

[11] Spier, op. cit.

[12] Pollmeier, op. cit.

Figure 4 shows the projected altitude error at Io versus data cutoff time for three specific data sets. The curve labeled Nominal is based on the standard S-band data models. The filled squares at the bottom of the plot denote days when pairs of regular ΔDOR measurements are scheduled, one measurement per baseline. The orbit analysis includes seven pairs of ΔDOR measurements prior to Io–50 days. The curve labeled Demo 1 cm includes the extra Δ DOR measurements listed in Table 3 (denoted by filled triangles in Fig. 4). The projected altitude error is reduced after the Io–50 days. The curve labeled Demo 1 cm includes the extra Δ DOR measurements listed in Table 3 (denoted by filled triangles in Fig. 4). The projected altitude error is reduced after the demonstration measurements until a few days before Io encounter, when the onboard optical data become dominant. The curve with All ΔDOR 1 cm is for the case where the regularly scheduled measurements are treated as high-precision measurements. The projected altitude error is reduced from the Nominal curve until the final few days.

VII. Effect of the Jupiter Ephemeris Error

Inclusion of the Earth–Jupiter and Galilean satellite ephemerides in the estimation list makes it difficult to see what improvement is taking place with changes in data. Analyses were performed with some of the estimated parameters removed to discover which estimated error sources were most important. Table 7 lists the computed errors when one of the following was removed from the estimation list: the Earth–Jupiter ephemeris, the radial stochastic spacecraft acceleration, or the Galilean satellite ephemerides. The data sets used were from the Nominal S-band, Demo-1-cm S-band, and All-ΔDOR-1-cm cases. The considered errors are not listed since changing the estimation list also changes the computed error and the effect of considered parameters.

In Table 7, the standard set estimates all parameters listed in Table 1. The next line lists the computed errors with the Galilean satellite ephemerides parameters removed from the estimation list. This produced little change in the $B \cdot T$ and LTOF errors, but the $B \cdot R$ error is reduced by a factor of two, although this error is not significant. The third line differs by the removal of the stochastic radial acceleration from the estimation list. However, it does include the satellite ephemerides. Dropping the stochastic acceleration improves the computed error by 20 to 30 percent depending on the data. But the stochastic radial acceleration is not the dominant error and does not prevent improved ΔDOR data from improving the orbit determination. The fourth and final line in Table 7 shows the effect of deleting the joint Earth–Jupiter ephemeris from the estimation list, while retaining the stochastic and satellite ephemeris. The computed errors are drastically reduced and improved ΔDOR data have little effect on the solution.

Examination of the estimated Earth and Jupiter state errors shows that the main error is in the down-track Jupiter error. Figure 5 shows the estimated Jupiter down-track error at several times. The nominal data improve the down-track error by 35 percent at the Io–19-day cutoff. Improved ΔDOR data significantly improve the down-track error but have almost no effect in the out-of-plane error. The estimated Earth state is better known than the Jupiter state and is not affected by the improved ΔDOR data.

VIII. Conclusion

This study has treated local-frame ΔDOR measurements as regular ΔDOR measurements with improved accuracy. It has shown that more accurate VLBI data improve orbit-determination accuracy. For the Galileo approach to Io, the errors in both the LTOF and $B \cdot T$ components are reduced significantly, with the latter error corresponding to the error in altitude above Io. Two ΔDOR measurements per baseline, with an accuracy of 1 cm, can produce an altitude accuracy improvement from 250 to 150 km at 19 days before Io encounter. A larger number of high-precision ΔDOR measurements can produce a factor of four improvement in altitude determination. Thus, improved ΔDOR measurements have the potential to greatly improve spacecraft navigation. Galileo's approach to Io provides a good opportunity to demonstrate that capability. The proper treatment of errors for high-precision VLBI measurements has yet to be determined. That includes determining which parameters are estimated as part of the measurement and which are included in the orbit-determination estimation. And there are still outstanding questions to be answered regarding reference-frame definition, nutation-series compatibility, and treatment of media and station errors, among other concerns.

Acknowledgments

The author thanks F. T. Nicholson, V. M. Pollmeier, D. W. Murrow, M. H. Finger, R. N. Treuhaft, and J. M. Davidson for their input and cooperation during the course of this study.

References

[1] J. S. Border, F. F. Donovan, S. G. Finley, C. E. Hildebrand, B. Moultrie, and L. J. Skjerve, "Determining Spacecraft Angular Position With Delta VLBI: The Voyager Demonstration," AIAA/AAS Astrodynamics Conference, San Diego, California, August 9–11, 1982.

[2] R. N. Treuhaft, "Deep Space Tracking in Local Reference Frame," *TDA Progress Report 42-94*, vol. April–June, Jet Propulsion Laboratory, Pasadena, California, pp. 1–15, July 15, 1988.

[3] J. K. Miller and K. H. Rourke, "The Application of Differential VLBI to Planetary Approach Orbit Determination," *DSN Progress Report 42-40*, vol. May and June, Jet Propulsion Laboratory, Pasadena, California, pp. 84–90, May 1977.

[4] R. A. Preston, D. D. Morabito, J. G. Williams, J. Faulkner, D. L. Jauncey, and G. D. Nicolson, "A VLBI Survey at 2.29 GHZ," *Astronomical Journal*, vol. 90, pp. 1599–1641, 1985.

[5] G. J. Bierman, *Factorization Methods for Discrete Sequential Estimation*, Orlando, Florida: Academic Press, 1977.

Table 1. Estimated and considered error terms

Estimated parameters	
Parameter	a priori error
Spacecraft position	10^8 km
Spacecraft velocity	10^8 km/sec
Constant radial acceleration	10^{-12} km/sec^2
Stochastic radial acceleration	10^{-12} km/sec^2 (a 5-day time constant)
Correction maneuvers	10^{-5} km/sec each direction
Earth ephemeris	24 m radial 21 km down track 28 km cross track
Jupiter ephemeris	15 km radial 140 km down track 162 km cross track
Io ephemeris	5 km radial 36 km down track 22 km cross track

Considered parameters	
Parameter	a priori error
Station locations	75-cm spin radius 1-m longitude 10-m z-height 10-cm baselines
Radial solar pressure	0.171
Wet troposphere	4 cm
Dry troposphere	1 cm
Day ionosphere (S-band)	75 cm
Night ionosphere (S-band)	15 cm
Optical centerfinding errors	0.5 pixel, 0.5 line

Table 2. Nominal data schedule for Galileo approach

Data type	Weight	Time period	Schedule
Optical	0.5 pixel	Io–57 to Io	Approx. 1 per satellite per day
Range	1 km	Io–142 to Io–136	DSS 14,43 1 per pass
		Io–136 to Io–110	DSS 43 1 every other pass
		Io–110 to Io–98	DSS 14,43 1 per pass
		Io–97 to Io–60	DSS 43 1 every other pass
		Io–60 to Io	DSS 14,43 1 per pass
Doppler	1 mm/sec	Io–142 to Io–136	DSS 14,43,63 1 per hour per pass
		Io–136 to Io–110	DSS 43 1 per hour every other pass
		Io–110 to Io–98	DSS 14,43,63 1 per hour per pass
		Io–97 to Io–60	DSS 43 1 per hour every other pass
		Io–60 to Io	DSS 14,43,63 1 per hour per pass
ΔDOR	14 cm	Io–146 to Io–136	1 per baseline per week
		Io–136 to Io–60	1 per baseline per month
		Io–60 to Io	2 per baseline per week

Table 3. Schedule of extra ΔDOR measurements for local reference frame demonstration cases

Baseline	Date	Time	Cutoff
14–43	12-Nov-1995	23:36	
14–63	13-Nov-1995	17:42	
14–63	16-Nov-1995	17:32	
14–43	16-Nov-1995	23:23	
	18-Nov-1995	15:45	Io–19d 2h
14–43	20-Nov-1995	23:10	
14–63	21-Nov-1995	17:16	
14–63	24-Nov-1995	17:07	
14–43	24-Nov-1995	22:57	
	26-Nov-1995	15:45	Io–11d 2h

Table 4. Orbit-determination results for the Standard cases

Error breakdown for Io–19-day 2-hour cutoff									
	Nominal			Demo 3-cm ΔDOR			Demo 1-cm ΔDOR		
	$B \cdot R$, km	$B \cdot T$, km	LTOF, sec	$B \cdot R$, km	$B \cdot T$, km	LTOF, sec	$B \cdot R$, km	$B \cdot T$, km	LTOF, sec
Computed	20.0	248.4	18.9	19.3	199.0	15.2	19.3	157.9	12.1
Solar	0.4	12.6	1.0	0.3	9.5	0.7	0.2	0.5	0.5
Station	0.6	13.7	1.0	0.7	16.4	1.2	0.6	1.0	1.0
Media	0.9	50.5	3.8	1.1	52.9	4.0	1.3	37.5	2.8
Optical	3.1	6.8	0.7	3.2	11.6	1.1	3.3	12.8	1.2
Total	20.3	254.7	19.4	19.9	207.4	15.8	19.6	163.7	12.5
Error breakdown for Io–11-day 2-hour cutoff									
	Nominal			Demo 3-cm ΔDOR			Demo 1-cm ΔDOR		
	$B \cdot R$, km	$B \cdot T$, km	LTOF, sec	$B \cdot R$, km	$B \cdot T$, km	LTOF, sec	$B \cdot R$, km	$B \cdot T$, km	LTOF, sec
Computed	16.1	119.5	9.2	15.4	93.8	7.2	14.9	71.9	5.5
Solar	0.1	1.3	0.1	0.1	1.6	0.1	0.0	1.7	0.1
Station	0.3	8.1	0.6	0.4	4.1	0.3	0.4	5.6	0.4
Media	0.7	15.7	1.2	1.1	1.5	1.5	1.1	22.0	1.7
Optical	3.8	46.7	3.8	3.8	35.5	3.0	3.9	26.5	2.3
Total	16.6	129.5	10.0	15.9	102.2	7.9	15.5	80.0	6.2

Table 5. Orbit determination results for the improved Doppler cases

Error breakdown for Io–19-day 2-hour cutoff									
	Nominal			Demo 3-cm ΔDOR			Demo 1-cm ΔDOR		
	$B \cdot R$, km	$B \cdot T$, km	LTOF, sec	$B \cdot R$, km	$B \cdot T$, km	LTOF, sec	$B \cdot R$, km	$B \cdot T$, km	LTOF, sec
Computed	19.7	219.0	16.7	19.4	183.4	14.0	19.2	150.7	11.4
Solar	0.2	8.1	0.6	0.2	7.1	0.5	0.2	5.8	0.4
Media	1.0	30.3	2.3	1.3	52.3	4.0	1.2	41.4	3.1
Optical	3.3	29.1	2.4	3.3	24.3	2.0	3.3	19.3	1.7
Total	20.0	223.1	17.0	19.7	192.4	14.7	19.5	157.6	12.0
Error breakdown for Io–11-day 2-hour cutoff									
	Nominal			Demo 3-cm ΔDOR			Demo 1-cm ΔDOR		
	$B \cdot R$, km	$B \cdot T$, km	LTOF, sec	$B \cdot R$, km	$B \cdot T$, km	LTOF, sec	$B \cdot R$, km	$B \cdot T$, km	LTOF, sec
Computed	16.0	86.9	6.7	15.3	77.5	6.0	14.9	61.8	4.8
Solar	0.0	0.9	0.1	0.1	1.3	0.1	0.1	1.7	0.1
Media	0.6	4.9	0.4	0.9	11.3	0.9	0.9	15.5	1.2
Optical	3.7	42.7	3.5	3.7	35.0	2.9	3.8	23.5	2.0
Total	16.4	97.0	7.6	15.8	85.8	6.7	15.4	67.9	5.3

Table 6. Orbit determination results for the All-ΔDOR-1-cm cases

Error breakdown for Io–19-day 2-hour cutoff						
	Standard models			Modified models		
	$B \cdot R$, km	$B \cdot T$, km	LTOF, sec	$B \cdot R$, km	$B \cdot T$, km	LTOF, sec
Computed	18.8	65.4	5.0	18.8	65.4	5.0
Solar	0.2	6.9	0.5	0.2	6.9	0.5
Station	0.4	14.2	1.1	0.0	1.3	0.1
Media	2.7	42.3	3.2	0.0	0.4	0.0
Optical	3.1	16.2	1.4	3.1	16.2	1.4
Total	19.3	81.2	6.2	19.1	67.8	5.2
Error breakdown for Io–11-day 2-hour cutoff						
	Standard models			Modified models		
	$B \cdot R$, km	$B \cdot T$, km	LTOF, sec	$B \cdot R$, km	$B \cdot T$, km	LTOF, sec
Computed	15.0	41.9	3.2	15.0	41.9	3.2
Solar	0.1	5.4	0.4	0.1	5.4	0.4
Station	0.6	9.7	0.7	0.0	0.4	0.0
Media	1.2	36.3	2.8	0.0	0.4	0.0
Optical	3.9	15.7	1.4	3.9	15.7	1.4
Total	15.5	58.7	4.6	15.5	45.1	3.5

Table 7. Computed errors with individual variables removed

	Nominal			Demo 1-cm ΔDOR			All ΔDOR 1 cm		
	$B \cdot R$, km	$B \cdot T$, km	LTOF, sec	$B \cdot R$, km	$B \cdot T$, km	LTOF, sec	$B \cdot R$, km	$B \cdot T$, km	LTOF, sec
Computed errors for Io–19-day 2-hour cutoff									
Standard set	20.0	248.4	18.9	19.3	157.9	12.1	18.8	65.4	5.0
No satellites	11.6	247.3	18.8	10.2	155.9	11.7	9.3	57.0	4.7
No stochastic	19.3	171.0	13.0	18.9	115.9	8.7	18.7	52.9	4.0
No Jupiter	18.3	44.7	3.3	17.9	38.0	2.8	17.9	37.6	2.8
Computed errors for Io–11-day 2-hour cutoff									
Standard set	16.1	119.5	9.2	14.9	71.9	5.5	15.0	41.9	3.2
No satellites	8.8	113.2	8.7	6.0	67.1	5.3	5.9	34.0	2.8
No stochastic	15.9	61.8	4.6	14.9	39.1	2.9	14.9	33.4	2.4
No Jupiter	15.7	31.9	2.2	14.3	21.9	1.4	14.4	22.2	1.5

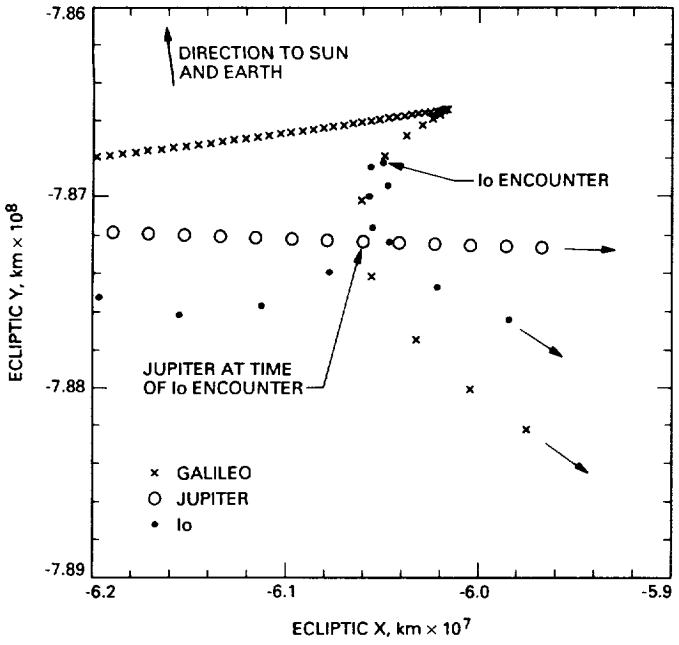

Fig. 1. Plot of the trajectories of Galileo, Jupiter, and Io in the ecliptic plane as seen by an inertial observer. Points are shown at four-hour intervals.

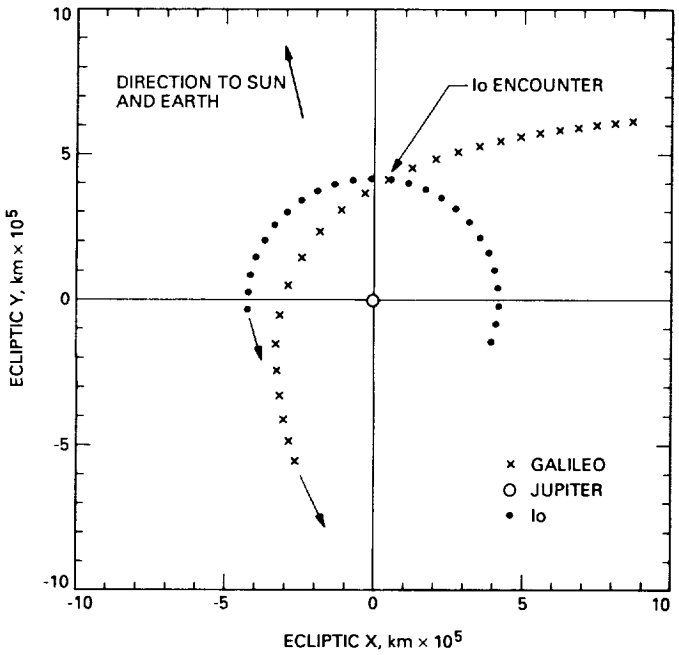

Fig. 2. Plot of the trajectories of Galileo, Jupiter, and Io in the ecliptic plane centered on Jupiter. Points are shown at one-hour intervals.

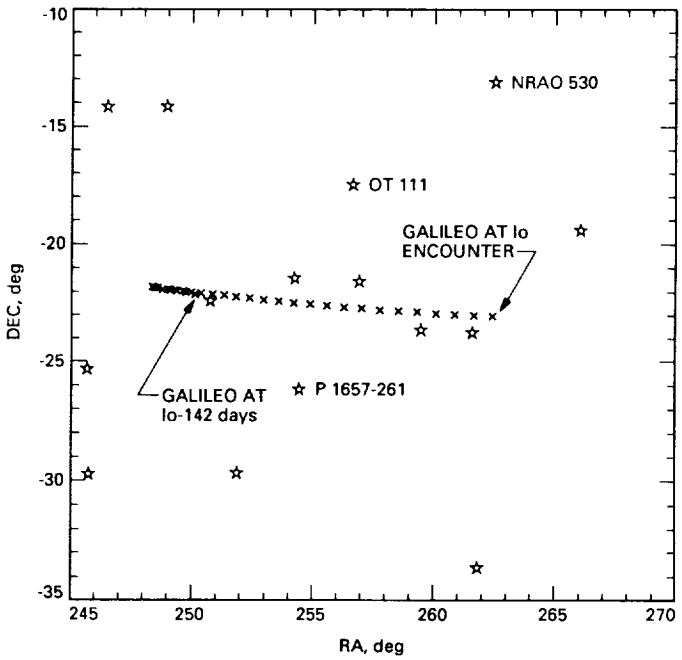

Fig. 3. Plot of the trajectory of Galileo in the plane of the sky. Points are shown at four-day intervals. The labeled radio sources are in the JPL Magellan catalog. The unlabeled sources are from the VLBI survey of [4].

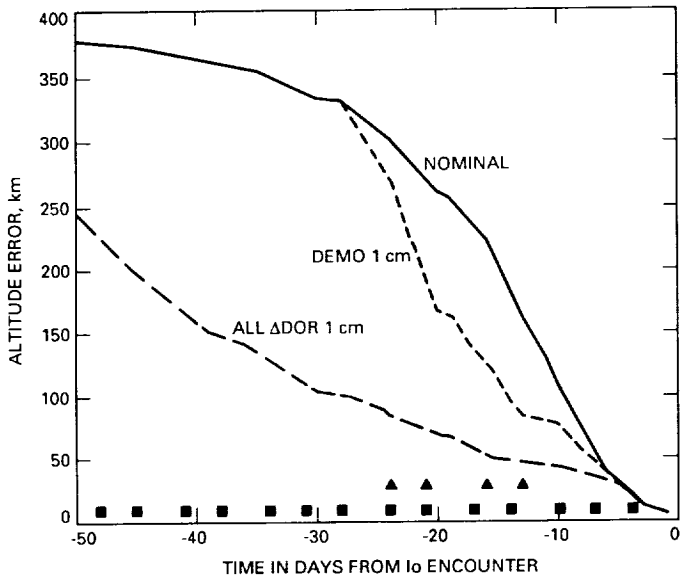

Fig. 4. Plot of the projected-altitude error at Io versus data-cutoff time for three data sets. The filled squares represent days when pairs of ΔDOR measurements are scheduled. The triangles show the times of the demonstration-measurement pairs.

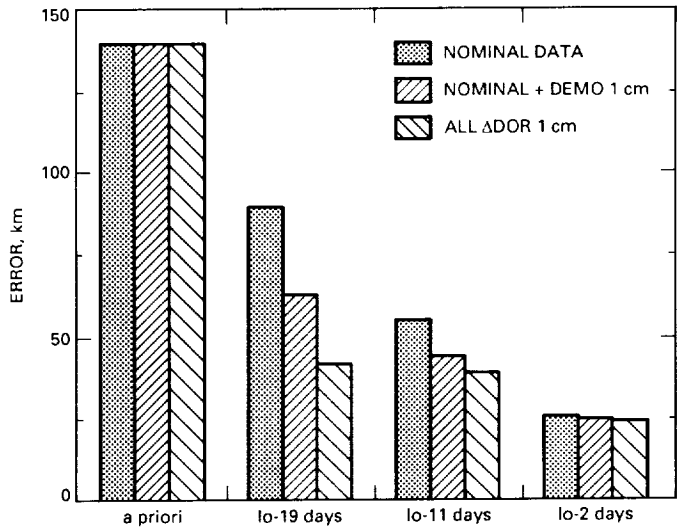

Fig. 5. The estimated Jupiter down-track error with different data sets.